Energy-Aware Radio Chip Management for Wireless Control

Nicolas Cardoso de Castro, Daniel E Quevedo, Federica Garin, Carlos Canudas de Wit

Energy-aware Radio Chip Management for Wireless Control

Nicolas Cardoso de Castro, Daniel E. Quevedo, *Senior Member, IEEE*, Federica Garin *Member, IEEE*, and Carlos Canudas-de-Wit, *Fellow, IEEE*.

***Abstract*—This paper addresses energy-aware control in a wireless control system. The goal is to save energy in a smart sensor node by co-designing its use of the radio chip together with the control policy. The focus is on exploiting the fact that in many radio-chips used in wireless nodes the depth of sleep can be manipulated dynamically. The choice of the mode involves a trade-off, since deeper sleep is cheaper to stay in, but leads to higher future transition costs. The opportunities arising from the use of multiple non-transmitting radio-modes have not been studied in the systems control literature. The present work presents a first step towards filling this gap. We propose a control scheme that manages the radio-modes of a single sensor node with computation capabilities. This *smart sensor* node is in charge of sensing the system state, computing the control law to be sent to the actuator, and managing its own radio chip. The joint optimization problem of finding the best switching policy for the radio-chip mode and the best feedback control law is obtained off-line using dynamic programming. The optimal policy is formulated over a finite horizon and implemented according to the model predictive control paradigm. Practical stability of the resulting control scheme is assessed and careful simulation studies document the potential energy savings that can be obtained with this technology.**

***Index Terms*—event-based control, dynamic programming, networked control, radio-chip mode management, energy efficient sensors**

I. Introduction

Networked Control Systems (NCS) are systems where the communication between the sensors, the controller and the actuators occurs through a network [1]. Energy is a key resource in those systems, in particular in wireless networks, where wireless nodes are often battery-driven. Energy-efficiency in wireless sensor networks has given rise to a rich literature, see *e.g.*, [2], [3], [4]. The bulk of this literature is focused on the transmission, regardless of the nature of the data or the final application. In a closed-loop system, the control performance is crucial, but has not been explicitly taken into account in most works focused on communications.

Part of this work was done during a visit of the first author to The University of Newcastle, supported by *Inria's Programme Explorateur*. This research was also partially supported under EU STREP project FeedNetBack FP7-ICT-2007-2.

N. Cardoso de Castro is with Karrus, F-38000 Grenoble, France (e-mail: nicolas.cardoso@karrus-its.com).

D. E. Quevedo is with the Department of Electrical Engineering, Paderborn University, 33098 Paderborn, Germany (e-mail: dquevedo@ieee.org).

F. Garin is with with Inria, Univ. Grenoble Alpes, CNRS, GIPSA-lab, F-38000 Grenoble, France (e-mail: federica.garin@inria.fr).

C. Canudas-de-Wit is with CNRS, GIPSA-lab, F-38000 Grenoble, France (e-mail: carlos.canudas-de-wit@gipsa-lab.fr).

On the other hand, in the systems and control community, there has been an active interest in saving energy in wireless NCS. Two research lines have emerged, which seek to reduce the amount of communications needed to achieve a given control objective. On the one hand, there have been studies on the minimum data-rate required to control a system, aiming at reducing the number of bits transmitted at each sampling time, see [5]. On the other hand, the number of transmissions can be reduced, by moving from periodic schemes, where a control action is transmitted and actuated based on periodic sampling, to event-based control, where a control action is transmitted only when needed. This means that a control input is sent and applied to the system only when a given event occurs; for instance, only if the system crosses a given threshold around the equilibrium point. A rich literature has emerged on event-based control, and this is still an active research area, see the surveys [6], [7] and references therein.

Most of the literature addresses communication and control problems separately. Interestingly, the works [8], [9] illustrate that further energy can be saved in control applications by a multi-layer approach. Here, two or more of the four layers relevant for NCSs are designed: physical layer, in charge of the radio modulation; data-link (MAC) layer, managing transmissions; network layer, routing data to destination; application layer, related to the overall control scheme. Few works consider the challenge of co-designing various layers. The two papers [10], [11] highlight the lack of a communication protocol dedicated to NCS, and derive suitable new protocols, which expose useful parameters to the application layer, so that a desired trade-off between reliability/latency and control performance can be found. The work [12] studies a state estimator that accounts for packet loss probabilities which depend upon time-varying channel gains, packet lengths and transmission power levels of the sensors; by adapting the source coding scheme and the transmission level at the sensor side, one can trade off energy and estimation performance. A communications and control co-design method is proposed in [13], [14]. Here, an optimization problem is formulated, describing both the control objective and the cost of transmissions. The goal in these works is to transmit only when needed (as in event-based control) and moreover to adjust the transmission power, which affects the packet drop probability and hence the control performance. A related problem is addressed in [15], where the effects of transmission power on packet drops are carefully modeled for the IEEE 802.15.4 protocol; then a constrained optimization problem is studied,

where the objective function is the energy consumption of the network, while the constraints are thresholds for the packet loss probability and delay, thereby ensuring a desired control quality. In [16], the authors compare wireless network implementations of various aperiodic-sampling control policies, by taking into account implementation issues in full detail. To be more specific, in [16] the authors build a wireless architecture based on the IEEE 802.15.4 protocol, and consider co-design of the aperiodic control, the wireless MAC protocol and the scheduling algorithm; they achieve low energy consumption by carefully switching off components for as much time as possible, *e.g.*, using a self-triggered technique [17]. The authors of [18] consider the case where the wireless communication is multi-hop, exploiting relay nodes in addition to sensor and controller nodes. They design the optimal joint policy for the controller and for the multi-hop forwarding policy, with energy as a constraint; their approach is based on decomposing the problem into two subproblems, transmission scheduling for maximizing the deadline-constrained reliability, and optimal control under packet loss.

In this paper, we investigate energy saving by communication and control co-design, focusing our attention on the radio chip of the wireless nodes. To limit the number of transmissions, our method transmits a control input only when necessary. Further, we propose to manage the radio-mode when it is not transmitting. Indeed, radio chips allow for intermediate modes between `Tx` and `Sleep`: When a node is not transmitting, its radio can be switched to one of its several non-transmitting (low-consuming) radio-modes. The management of the radio chip modes can lead to interesting energy savings [3], [4], and management in accordance with the needs of a control application is a non-trivial and to date unexplored problem.

Our main technical contribution consists in considering several low-consuming radio-modes in an optimal control problem. Our strategy is a joint design of the radio-mode switching policy and the feedback control law used to govern the system actuators. We adopt a finite horizon optimal control framework. The optimization problem is solved using dynamic programming, with the value iteration method. This paper extends our previous work [19] by giving detailed proof of the stability results, introducing a more detailed system description, and including new simulation studies.

The remainder of this manuscript is organized as follows: in Section II, we describe the system and we introduce the problem of interest. In Section III, we give a mathematical formulation of the problem as a finite-horizon optimization; then we propose a solution, based on dynamic programming, to be run off-line to obtain a jointly optimal feedback law and radio-mode switching policy; finally we discuss the implementation of the feedback law and radio-mode switching policy over a receding horizon. Section IV establishes stability results of the derived scheme in the framework of Input-to-State Stability. Simulation results are included in Section V. Section VI draws conclusions.

II. Feedback control with a smart sensor

A. Problem description

We focus our attention on a setup composed of two nodes, as depicted in Fig. 1 and described hereafter.[1] The first node, called the smart sensor node, has sensing and computing capabilities. It is in charge of sensing the system state, computing the control input and deciding whether or not to send the control input to the second node. The latter is in charge of applying the control input to the actuator. The smart sensor is an autonomous wireless node powered by a battery. A wireless channel is located between the smart sensor node and the actuator node. The actuator node is co-located with the actuator. This node has access to an unlimited energy source since the actuator itself (*e.g.*, a motor, a solenoid valve) generally needs a relevant amount of energy. Then, our focus is on saving energy at the smart sensor side. This configuration, also called *one-channel feedback NCS*, is often considered in the literature, see *e.g.*, [1]. The effects of the channel, such as packet dropouts, errors, and delays, have been widely studied. In this paper, our focus is on energy consumption and on the use of non-periodic transmissions. For simplicity, we assume an ideal channel, where all transmitted messages are received correctly and timely.[2]

Energy can be saved at the smart sensor not only by limiting the amount of communication, but also by a suitable choice of the low-consuming radio-mode when no transmission occurs. Low-consuming radio-modes are described in Subsection II-B. They correspond to partial use of the radio components, while the sensing and computing units are always operating.

We consider an optimal control formulation, which leads to event-based communication, on the base of discrete-time monitoring. This means that the smart sensor monitors the system at a given sampling period. At each sampling instant, depending on the state of the system, the smart sensor decides if a transmission occurs at the current time. This is the same setup as in *periodic event-based control* [21]. In comparison to continuous-time monitoring, this is better suited for practice. Moreover it avoids theoretical subtleties such as Zeno behaviors.

When a transmission occurs, the smart sensor also decides the control input to be sent to the actuator. At instances where no transmission occurs, the smart sensor decides on a low-consuming radio-mode to switch to. Our goal is the joint optimization of the transmission pattern, of the feedback control to be sent to the actuator (when a transmission occurs), and of the choice of the low-consuming radio-mode (when no transmission occurs).

B. Radio modes

Low-consuming modes are non-transmitting modes. They allow one to save energy by turning off some components

[1] A two-nodes setup captures the challenges of energy efficiency without introducing the difficulties appearing in a multi-nodes setup (such as medium access control or routing).

[2] For event-based control over unreliable communication channels, see, *e.g.*, [20]

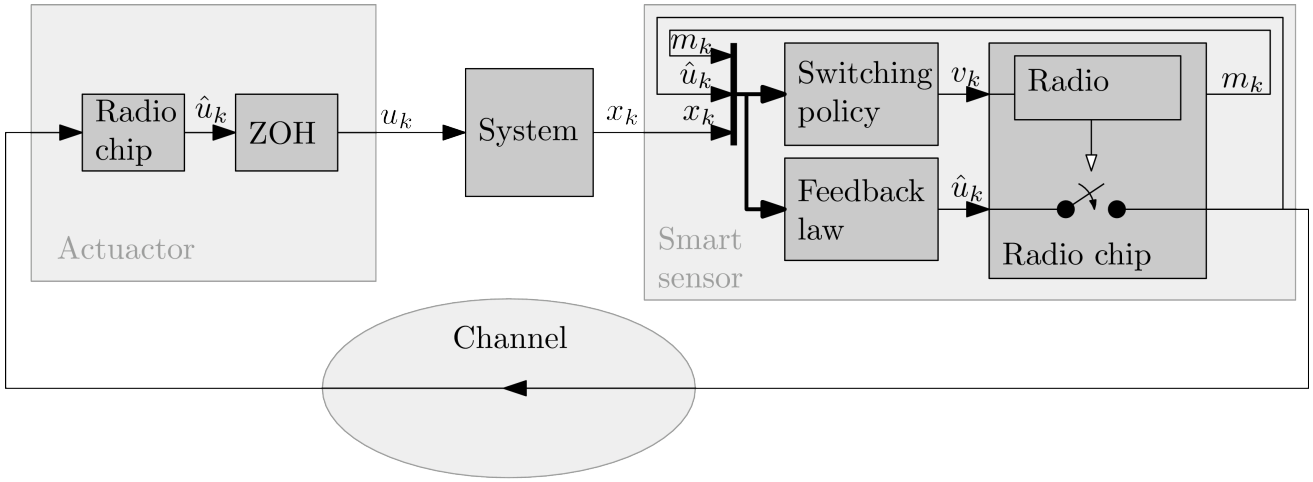

Fig. 1. The smart sensor node measures the system state x_k. It decides whether to send a feedback control input to the actuator node. If controlling is chosen, then it sends the feedback $\hat{u}_k$. If not, it manages the mode of the radio chip, by selecting a low-consuming mode. The transmission channel is ideal, and the receiver is able to determine if it has received a value or not.

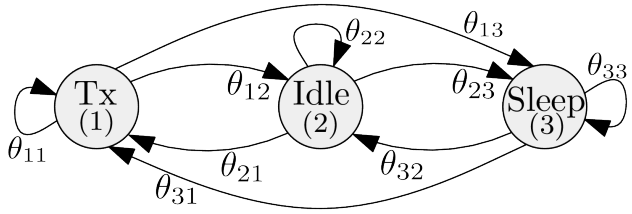

Fig. 2. Illustration of the transition costs with $N = 3$. `Idle` is an intermediate mode between the transmitting mode and the `Sleep` mode. Arrows represent transitions, labeled with their costs.

in the radio chip, such as the frequency synthesizer, the crystal oscillator, or the voltage regulator (see [3], [4] for details). Time and energy are needed to switch between modes, depending on the depth of sleep, *i.e.*, the amount of components that are turned off. Switching delays are usually not an issue, being often smaller than the sampling time of the dynamical system. Energy, however, is crucial. Physical details of the radio-modes are application-dependent. Here, we give a high-level description, aggregating in transition costs all the information we need about the energy consumption.

We denote with N the number of radio-modes; we consider one transmitting mode and $N-1$ non-transmitting modes.[3] The state of the radio chip of the smart sensor is the radio-mode at time k, denoted by

$$m_k \in \mathbb{M} \triangleq \mathbb{M}_1 \cup \mathbb{M}_2,$$

where $\mathbb{M}_1 \triangleq \{1\}$ is the set containing the transmitting mode, and $\mathbb{M}_2 \triangleq \{2, 3, \cdots, N\}$ is the set of non-transmitting modes. A radio chip can be modeled by an automaton (as the one depicted in Figure 2 in the case of $N = 3$), with N states describing the radio mode (*e.g.*, $1 =$ `Tx`, $2 =$ `Idle`, and $3 =$ `Sleep`), and transition costs modeling energy used for radio-mode switching. We model the behavior of the radio chip at each sampling instant. Since the monitoring of the system is periodic, the decision to send a control update (and then to change the state of the radio) is also periodic. At each sampling instant, the sensor node is in a state i and has to choose the next state j of the automaton, paying the cost θ_{ij} associated with changing state (or staying in the current state, if $j = i$). We will denote with E_k the amount of energy consumed since the commissioning up to time k. Initializing $E_0 = 0$, we thus obtain

$$E_{k+1} = E_k + \theta_{m_k, m_{k+1}}.$$

We also introduce the convention to order the modes according to their energy costs, namely

$$\theta_{1,1} > \theta_{2,2} \geq \ldots \geq \theta_{N,N} \geq 0.$$

Transition costs need to be computed by taking into account the sampling time and the details of the radio-chip at hand. This includes all the steps to be done at the radio level for the transition, including their duration and energy cost, and then also the cost to stay in the new mode until the end of the sampling time. In our current work, we have focused on the following example.

Example 1. *We consider the CC1100 transreceiver from Texas Instruments [22]. We define an intermediate* `Idle` *mode in between* `Tx` *and* `Sleep` *modes and we compute the transition costs for a sampling time of* 5 *ms. The modes at the radio chip level (*e.g.*, Sleep, Idle, Calibrate, FastTX, RXoverflow) are different from the high-level ones that we want to expose to the control application. Hence, the transition costs must take into account a composition of actions done at the radio level, each with its time duration and its current consumption, thereby resulting in an overall energy expenditure. As an example, the computation of* $\theta_{3,3}$ *(*i.e.*, the cost to stay in the* `Idle` *mode for a sampling time) is straightforward from the values of the current drawn in this mode (*400 *nA from [22, Table 4]), the chip voltage (*3.0 *V from [22, Table 4]) and the time spent (a sampling period of* 5 *ms). The product of these three values gives* $\theta_{3,3} = 60$ *nJ. To characterize other transition costs, more*

[3] Alternative works, such as [12], [13], [14], focus on controlling multiple transmitting modes and aggregate all the non-transmitting modes into a single mode.

careful computations are needed. For instance, switching from `Sleep` *to* `Idle` *needs to consider the time spent to turn on the crystal oscillator, namely,* 0.15 *ms [22, Table 7]) using* 8.2 *mA [22, Table 4]). Further, a calibration is needed before any transmission when the sleep mode has been activated. Also, when all operations for the transition are shorter than the sampling time, one needs to also account for the time spent in the mode after having reached it.*

Taking into account the above, the following costs are obtained, given in mJ*:*

$$\begin{array}{lll} \theta_{1,1}=2.9, & \theta_{1,2}=1.8, & \theta_{1,3}=1.9, \\ \theta_{2,1}=3.2, & \theta_{2,2}=1.4, & \theta_{2,3}=6\cdot 10^{-5} \\ \theta_{3,1}=3.5, & \theta_{3,2}=3.75\cdot 10^{-3}, & \theta_{3,3}=6\cdot 10^{-5}. \end{array}$$

As noted before, our approach considers several non-transmitting modes in order to save further energy than when using a simple `On`/`Off` pattern. However, because of transition costs, in some cases switching to intermediate non-transmitting modes may result in more energy waste than holding a transmitting mode. Our approach will effectively reduce the energy consumption, only under some assumptions on the transition costs.

Assumption 1. *The energy cost to stay in the transmitting mode is positive and larger than the cost of staying in any non-transmitting mode:* $0 \leq \theta_{i,i} < \theta_{1,1}$ *for all* $i \in \mathbb{M}_2$*. All transitions between distinct states have positive cost:* $\theta_{i,j} > 0$ *for all* $i \neq j$*.*

Assumption 2. *The transition from (and to) the transmitting mode is larger when considering a deeper non-transmitting modes: For any* $i, j \in \mathbb{M}_2$*, if* $i < j$ *(*i.e.*,* $\theta_{i,i} \geq \theta_{j,j}$*,) then* $\theta_{1,i} \leq \theta_{1,j}$ *and* $\theta_{i,1} \leq \theta_{j,1}$*.*

Assumption 1 is quite natural, since a deeper mode has more components switched off. However, there is no guarantee that Assumption 2 is always satisfied, due to the fact that $\theta_{i,j}$ represents the energy consumed over an entire sampling interval, including the cost to remain in the mode after having reached it.

III. Optimal co-design of radio-modes and feedback control

Our goal is to find suitable policies both for the radio-mode of the smart sensor and for the feedback control law. Thereby, we seek to obtain a satisfying trade-off between the control performance and the energy consumption. In this section, after giving a detailed mathematical description of the system, we formulate an optimization problem with the minimization of a cost function that accounts for the control performance and the energy consumed by the radio, as modeled in Subsection II-B. The minimization problem is solved offline with dynamic programming. The optimization is over a finite horizon, but the closed-loop system is implemented online using Model Predictive Control ideas. Indeed, the offline procedure provides a feedback sequence and mode-switching sequence over the finite horizon for any initial state of the system state space. On-line, only the first element of each sequence is used and the procedure is repeated *ad-infinitum*. The notion of receding horizon is mainly used in model predictive control, see, e.g., [23], [24] for background on this topic.

A. Mathematical model

1) System model: The system to be controlled is a linear discrete-time system:

$$x_{k+1} = Ax_k + Bu_k, \tag{1}$$

where x_k is the system state (fully observed, for simplicity) and u_k is the control input taking values in $\mathbb{R}^{n_x}$ and $\mathbb{R}^{n_u}$ respectively. The system is controllable, and may be unstable. Our goal is to stabilize this system around the origin, $x_k = \mathbf{0}$, while saving energy.

2) Channel model: The channel is considered here as perfect, *i.e.*, if a control input $\hat{u}_k$ is sent by the smart sensor, then it is correctly received by the actuator node.

3) Switching policy and feedback law: The sensor node embeds a switching policy η (whose joint-design with the feedback law μ will be described hereafter) to govern the radio-mode. The decision to switch between modes is based on the overall system state, comprising x_k, the last control input u_{k-1} applied to the system and the current radio-mode, denoted m_k. Denoting the memory of the last control input by

$$\tilde{u}_k = u_{k-1}, \tag{2}$$

the switching decision is given by $v_k = \eta(x_k, \tilde{u}_k, m_k)$. The smart sensor has perfect knowledge of the last control input applied to the system (since any update sent to the actuator node is indeed received and applied to the system). The radio-mode is updated according to the switching decision: $m_{k+1} = v_k$.

The control input applied to the system, denoted u_k, depends on the arrival of the update $\hat{u}_k$, which in turn depends on the decision to send an update. If an update is received, then the optimal control input is used, as computed by the smart sensor according to the law described in the next section, denoted $\hat{u}_k = \mu(x_k, \tilde{u}_k, m_k)$. Otherwise, the control input is held to its previous value as long as no update is received from the smart node:

$$u_k = \begin{cases} \hat{u}_k, & \text{in case of transmission,} \\ u_{k-1}, & \text{otherwise.} \end{cases} \tag{3}$$

4) Switched model: The evolution of the system under the different choices of radio-mode can be formulated as a switched linear system with N modes. From a control point of view, the different modes are actually reduced to two cases: when a transmission occurs (*i.e.*, the control loop is closed) and when the system runs open loop. However the different modes affect the energy consumption. Choosing the switching policy at time k is equivalent to choosing the radio-mode. The evolution of the switched system depends on x_k, on $\tilde{u}_k$, and on m_k, the mode of the radio chip. Accordingly, we define

z_k as the system state augmented with the control memory $\tilde{u}_k$ defined in Eq. (2):

$$z_k = \begin{bmatrix} x_k \\ \tilde{u}_k \end{bmatrix} \in \mathbb{R}^{n_x+n_u}.$$

Then, the state of the switched system becomes:

$$(z_k, m_k) \in \mathbb{X} \triangleq \mathbb{R}^{n_x+n_u} \times \mathbb{M}.$$

The evolution of the system in Eq. (1) with the feedback law μ described in Eq. (3), together with the radio-mode switching policy η, gives rise to the following switched system:

$$\begin{cases} z_{k+1} = f_{v_k}(z_k, \hat{u}_k) \\ m_{k+1} = v_k = \eta(z_k, m_k) \\ \hat{u}_k = \mu(z_k, m_k), \end{cases} \tag{4}$$

where the function f_{v_k} is defined as

$$f_{v_k}(z_k, \hat{u}_k) \triangleq \Phi_{v_k} z_k + \Gamma_{v_k} \hat{u}_k,$$

and the matrices Φ_{v_k}, Γ_{v_k}, for $v_k \in \mathbb{M}$, are as follows:

1) if $v_k = 1$, *i.e.*, if a transmission occurs, then

$$\Phi_{v_k} = \Phi_{CL} = \begin{bmatrix} A & \mathbf{0} \\ \mathbf{0} & \mathbf{0} \end{bmatrix}, \quad \Gamma_{v_k} = \Gamma_{CL} = \begin{bmatrix} B \\ \mathbf{I} \end{bmatrix},$$

2) if $v_k \in \mathbb{M}_2$, *i.e.*, if there is no transmission, then

$$\Phi_{v_k}(\beta_k) = \Phi_{OL} = \begin{bmatrix} A & B \\ \mathbf{0} & \mathbf{I} \end{bmatrix}, \quad \Gamma_{v_k}(\beta_k) = \Gamma_{OL} = \begin{bmatrix} \mathbf{0} \\ \mathbf{0} \end{bmatrix}.$$

B. Finite-horizon optimization problem

We define a stage cost (or cost-to-go), $\ell_{v_k}(z_k, m_k, u_k)$ as a joint criterion capturing the feedback performance and the energy consumed by the sensor over one sampling interval:

$$\ell_{v_k}(z_k, m_k, u_k) = \underbrace{x_k^\top \bar{Q} x_k}_{\text{performance}} + \underbrace{u_k^\top \bar{R} u_k}_{\text{control energy}} + \alpha \underbrace{\theta_{m_k v_k}}_{\text{transmission energy}}, \tag{5}$$

for symmetric positive definite matrices $\bar{Q}$ and $\bar{R}$, and for a parameter α. The latter can be tuned to give different trade-offs between feedback performance and energy consumption.

This stage cost can be expressed in the switched formulation, as follows:

$$\ell_{v_k}(z_k, m_k, u_k) = z_k^\top Q_{v_k} z_k + u_k^\top R_{v_k} u_k + \alpha \theta_{m_k v_k}, \tag{6}$$

where the matrices Q_{v_k} and R_{v_k}, for $v_k \in \mathbb{M}$, are as follows:

1) if $v_k = 1$, then

$$Q_{v_k} = Q_{CL} = \begin{bmatrix} \bar{Q} & \mathbf{0} \\ \mathbf{0} & \mathbf{0} \end{bmatrix}, \quad R_{v_k} = R_{CL} = \bar{R},$$

2) if $v_k \in \mathbb{M}_2$, then

$$Q_{v_k} = Q_{OL} = \begin{bmatrix} \bar{Q} & \mathbf{0} \\ \mathbf{0} & \bar{R} \end{bmatrix}, \quad R_{v_k} = R_{OL} = \mathbf{0}.$$

The cost function is defined as the sum of the stage costs over a finite-horizon of length H:

$$\begin{aligned} &J_H(z_k, m_k, \mathcal{U}_{k,H}, \mathcal{V}_{k,H}) \\ &\quad = \sum_{i=k}^{k+H-1} \ell_{v_i}(z_i, m_i, u_i) + z_{k+H}^\top Q_F z_{k+H}, \end{aligned} \tag{7}$$

where

$$\mathcal{U}_{k,H} \triangleq (u_k, \ldots, u_{k+H-1})$$
$$\mathcal{V}_{k,H} \triangleq (v_k, \ldots, v_{k+H-1})$$

are the control and switching sequences along the horizon, and the symmetric positive definite matrix Q_F is a weighting factor on the final augmented state at the end of the horizon.

The optimization problem consists in finding the optimal control policy sequence $\mathcal{U}_{k,H}^*$ and the optimal switching policy sequence $\mathcal{V}_{k,H}^*$ that minimize the cost function in Eq. (7):

$$\begin{aligned} J_H^*(z_k, m_k) &\triangleq J_H(z_k, m_k, \mathcal{U}_{k,H}^*, \mathcal{V}_{k,H}^*) \\ &= \min_{\mathcal{U}_{k,H}, \mathcal{V}_{k,H}} J_H(z_k, m_k, \mathcal{U}_{k,H}, \mathcal{V}_{k,H}), \end{aligned} \tag{8}$$

where superscripts * refer to the optimal values.

Remark 1 (Time-invariance)**.** *It is worth noting that the problem is time invariant, which means that the control inputs and switching decisions depend on the current state (z_k, m_k) and on the horizon length H, but not on k. It is thus sufficient to solve the problem with the state as a parameter.*

C. Dynamic programming solution

The optimal sequences, $\mathcal{U}_{k,H}^*$, $\mathcal{V}_{k,H}^*$, defined in Eq. (8) can be computed using dynamic programming with the value iteration method (see [25], [26], [27]). The problem being time invariant, it is sufficient to find a solution parametrized in the current state (z_k, m_k). The value iteration method defines a value function $V_H(z_k, m_k)$ which is given by the following recursion: the value function is initialized as

$$V_0(z_{k+H}, m_{k+H}) = z_{k+H}^\top Q_F z_{k+H} \tag{9}$$

and then, for all $i = 1, \ldots, H$,

$$\begin{aligned} &V_i(z_{k+H-i}, m_{k+H-i}) \\ &= \min_{u_{k+H-i}, v_{k+H-i}} \left\{ \ell_{v_{k+H-i}}(z_{k+H-i}, m_{k+H-i}, u_{k+H-i}) \right. \\ &\qquad \left. + V_{i-1}(f_{v_{k+H-i}}(z_{k+H-i}, u_{k+H-i}), v_{k+H-i}) \right\}. \end{aligned} \tag{10}$$

This method gives the optimal solution

$$J_H^*(z_k, m_k) = V_H(z_k, m_k).$$

It turns out that in our case, the value function takes the explicit form:

$$V_i(z_k, m_k) \triangleq \min_{(\Pi, \boldsymbol{\pi}) \in \mathcal{P}_i} \left\{ z_k^\top \Pi z_k + \pi_{m_k} \right\}, i \in \{0, 1, \ldots, H\}, \tag{11}$$

where $\mathcal{P}_i$ is a set of pairs $(\Pi, \boldsymbol{\pi})$, where Π is a square matrix of dimension $n_x + n_u$ and $\boldsymbol{\pi}$ is a vector of dimension N. π_i refers to the i^{th} component of the vector $\boldsymbol{\pi}$.

Indeed, when $i = 0$, Eq. (9) implies that $V_0(z_{k+H}, m_{k+H})$ satisfies Eq. (11) with $\mathcal{P}_0 = \{(Q_F, \mathbf{0})\}$.

Then, for $0 < i \leq H$, and assuming that:

$$\begin{aligned} &V_{i-1}(z_{k+H-i+1}, m_{k+H-i+1}) \\ &= \min_{(\Pi, \boldsymbol{\pi}) \in \mathcal{P}_{i-1}} \left\{ z_{k+H-i+1}^\top \Pi z_{k+H-i+1} + \pi_{m_{k+H-i+1}} \right\}, \end{aligned} \tag{12}$$

we can compute $\mathcal{P}_i$ such that $V_i(z_{k+H-i}, m_{k+H-i})$ can be written in the same form. To ease the notation, we omit the index and we add the superscript $^-$ to denote the indices $i-1$, while the absence of a superscript refers to i. Recalling Eq. (10), we thus obtain:

$$\begin{aligned}V(z,m) &= \min_{u,v}\left\{\ell_v(z,m,u) + V^-(f_v(z,u),v)\right\}\\ &= \min_{u,v}\Big\{z^\top Q_v z + u^\top R_v u + \alpha\theta_{mv}\\ &\quad + \min_{(\Pi,\boldsymbol{\pi})\in\mathcal{P}^-}\left\{f_v(z,u)^\top \Pi f_v(z,u) + \pi_v\right\}\Big\}\\ &= \min_{u,v,(\Pi,\boldsymbol{\pi})\in\mathcal{P}^-}\Big\{z^\top(Q_v + \Phi_v^\top \Pi \Phi_v)z\\ &\quad + u^\top\big(R_v + \Gamma_v^\top \Pi \Gamma_v\big)u + 2u^\top\Gamma_v^\top\Pi\Phi_v z + \alpha\theta_{m,v} + \pi_v\Big\}.\end{aligned} \tag{13}$$

We shall use the fact that matrices Π are symmetric (this can be easily proved) and distinguish two cases. If $v = 1$, then Eq. (13) becomes:

$$\begin{aligned}V(z,m) = \min_{u,(\Pi,\boldsymbol{\pi})\in\mathcal{P}^-}\Big\{&z^\top(Q_{CL} + \Phi_{CL}^\top\Pi\Phi_{CL})z\\ &+ u^\top(R_{CL} + \Gamma_{CL}^\top\Pi\Gamma_{CL})u\\ &+ 2u^\top\Gamma_{CL}^\top\Pi\Phi_{CL}z + \alpha\theta_{m,1} + \pi_1\Big\}.\end{aligned} \tag{14}$$

We can compute separately

$$u^* \triangleq \arg\min_u \left\{u^\top(R_{CL} + \Gamma_{CL}^\top\Pi\Gamma_{CL})u + 2u\Gamma_{CL}^\top\Pi\Phi_{CL}z\right\},$$

by noting that

$$\begin{aligned}\frac{\partial}{\partial u}&\left(u^\top(R_{CL} + \Gamma_{CL}^\top\Pi\Gamma_{CL})u + 2u\Gamma_{CL}^\top\Pi\Phi_{CL}z\right)\\ &= \left(R_{CL} + \Gamma_{CL}^\top\Pi\Gamma_{CL}\right)u + \Gamma_{CL}^\top\Pi\Phi_{CL}z,\end{aligned}$$

so that

$$u^* = -\left(R_{CL} + \Gamma_{CL}^\top\Pi\Gamma_{CL}\right)^{-1}\Gamma_{CL}^\top\Pi\Phi_{CL}z \triangleq -K_\Pi z.$$

Replacing the value of u^* in Eq. (14) yields:

$$\begin{aligned}V(z,m) = \min_{(\Pi,\boldsymbol{\pi})\in\mathcal{P}^-}\Big\{&\alpha\theta_{m,1} + \pi_1\\ &+ z^\top\big(Q_{CL} + \Phi_{CL}^\top\Pi\Phi_{CL} + K_\Pi^\top\Gamma_{CL}^\top\Pi\Phi_{CL}\big)z\Big\}.\end{aligned} \tag{15}$$

In the second case, $v \in \mathbb{M}_2$, the control input is held to the previous value, see Eq. (3), and does not appear anymore in the minimization. Eq. (13) thereby reduces to:

$$\begin{aligned}V(z,m) = \min_{v\in\mathbb{M}_2,(\Pi,\boldsymbol{\pi})\in\mathcal{P}^-}\Big\{&z^\top(Q_{OL} + \Phi_{OL}^\top\Pi\Phi_{OL})z\\ &+ \alpha\theta_{m,v} + \pi_v\Big\}.\end{aligned} \tag{16}$$

From Eqs. (15)-(16), one can build $\mathcal{P}_i$ (where the details about the elements in the set are given in the following lemma) such that $V_i(z_{k+H-i}, m_{k+H-i})$ can be written in the same form as in Eq. (12). The above analysis leads to the following result:

Lemma 1. *The optimal cost function $J_H^*(z_k, m_k)$ that solves the problem* (8) *is given by:*

$$J_H^*(z_k,m_k) = V_H(z_k,m_k) \triangleq \min_{(\Pi,\boldsymbol{\pi})\in\mathcal{P}_H}\left\{z_k^\top\Pi z_k + \pi_{m_k}\right\} \tag{17}$$

where $\mathcal{P}_H$ is a set of pairs $(\Pi, \boldsymbol{\pi})$, with Π a square matrix of dimension n_x+n_u and $\boldsymbol{\pi}$ a vector of dimension N (whose jth entry is denoted by π_j). $\mathcal{P}_H$ is computed with the following recursion:

$$\begin{aligned}&\mathcal{P}_0 = \{(Q_F, \mathbf{0})\},\\ &\mathcal{P}_i = \mathcal{P}_i^1 \cup \mathcal{P}_i^2 \quad \forall i \in \{1,2,\ldots,H\},\end{aligned}$$

where

$$\kappa_\Pi = \left(R_{CL} + \Gamma_{CL}^\top\Pi\Gamma_{CL}\right)^{-1}\Gamma_{CL}^\top\Pi\Phi_{CL},$$

$$\mathcal{P}_i^1 = \left\{\left(Q_{CL} + \Phi_{CL}^\top\Pi\Phi_{CL} - \kappa_\Pi^\top\Gamma_{CL}^\top\Pi\Phi_{CL}, \begin{bmatrix}\alpha\theta_{1,1}+\pi_1\\ \alpha\theta_{2,1}+\pi_1\\ \vdots\\ \alpha\theta_{N,1}+\pi_1\end{bmatrix}\right)\right\}$$
$$\text{such that } (\Pi,\boldsymbol{\pi}) \in \mathcal{P}_{i-1}$$

and

$$\mathcal{P}_i^2 = \left\{\left(Q_{OL} + \Phi_{OL}^\top\Pi\Phi_{OL}, \begin{bmatrix}\min_{v\in\mathbb{M}_2}\{\alpha\theta_{1,v}+\pi_v\}\\ \min_{v\in\mathbb{M}_2}\{\alpha\theta_{2,v}+\pi_v\}\\ \vdots\\ \min_{v\in\mathbb{M}_2}\{\alpha\theta_{N,v}+\pi_v\}\end{bmatrix}\right)\right\}.$$
$$\text{such that } (\Pi,\boldsymbol{\pi}) \in \mathcal{P}_{i-1}$$

Recursively, for $i \in \{0,1,\ldots,H-1\}$, let:

$$(\Pi_{H-i}, \boldsymbol{\pi}_{H-i}) = \arg\min_{(\Pi,\boldsymbol{\pi})\in\mathcal{P}_{H-i}}\left\{z_{k+i}^\top\Pi z_{k+i} + \pi_{m_{k+i}}\right\}.$$

The optimal switching decision at time $k+i$ is given by:

$$v_{k+i}^* = \eta_i^*(z_{k+i}, m_{k+i}) \triangleq \begin{cases}1, \text{ if } (\Pi_{H-i},\boldsymbol{\pi}_{H-i}) \in \mathcal{P}_{H-i}^1\\ \arg\min_{v\in\mathbb{M}_2}\left\{\alpha\theta_{m_{k+i},v} + \pi_v\right\}, \text{ else.}\end{cases}$$

When $v_{k+i}^* = 1$, the optimal control input is given by:

$$u_{k+i}^* = \mu_i^*(z_{k+i}, m_{k+i}) \triangleq -\kappa_{\Pi_{H-i}} z_{k+i} = -K_{\Pi_{H-i}} x_{k+i}$$

where $\kappa_{\Pi_{H-i}} = \begin{bmatrix}K_{\Pi_{H-i}} & 0\end{bmatrix}$ and

$$K_{\Pi_{H-i}} = \left(R_{CL} + \Gamma_{CL}^\top\Pi_{H-i}\Gamma_{CL}\right)^{-1}\Gamma_{CL}^\top\Pi_i\Phi_{CL}.$$

The optimal control inputs and switching decisions over the horizon are then given by $\mathcal{U}_{k,H}^* = (u_k^*, u_{k+1}^*, \ldots, u_{k+H-1}^*)$ and $\mathcal{V}_{k,H}^* = (v_k^*, v_{k+1}^*, \ldots, v_{k+H-1}^*)$. □

It is worth emphasizing that the value iteration method only needs to be run offline. It provides the optimal decisions with the system state as a parameter. Online, the optimal switching decision and feedback control input are then derived for the current state of the system, as described below.

D. MPC implementation

While the offline procedure provides sequences of control inputs and switching decisions over a finite horizon H, an infinite horizon controller can be formulated by adopting a receding horizon approach. Only the first element of each sequence is used at a time k, and the optimal sequences over the horizon H are computed again at the next sampling instant $k+1$. This allows one to define the joint switching policy and feedback law that we use online (μ^*, η^*) as defined in the switched formulation in Eq. (4) as the first laws in the sequences obtained from the value iteration method:

$$\begin{cases} \mu^*(z_k, m_k) = \mu_0^*(z_k, m_k) \\ \eta^*(z_k, m_k) = \eta_0^*(z_k, m_k). \end{cases} \tag{18}$$

As noted above, our scheme can be divided into an offline computation and an online computation part. The joint policy (μ^*, η^*) is computed offline. Then the following algorithm is run online on the smart node at each sampling time:
Find the switching decision, i.e.*, the next radio-mode,* $m_{k+1} = v_k^* = \eta^*(z_k, m_k)$ *and*

- *if* $v_k^* \in \mathbb{M}_1$*, find the optimal control input* $u_k^* = \mu^*(z_k, m_k)$ *and send it to the actuator,*
- *if* $v_k^* \in \mathbb{M}_2$*, do nothing.*

Interestingly, our optimization leads to an event-based control law, where the mode switching policy η triggers control updates based on the current state (z_k, m_k). Indeed, the space $\mathbb{X}$ is divided into regions whose crossings trigger events, in a similar manner that threshold crossings trigger events in event-based control [7]. Our approach is related to works on event-triggered model predictive control, such as [28], [29], except that our method includes management of multiple radio-modes.

The solution of the optimization problem as given in Lemma 1 provides an optimal feedback sequence $\mathcal{U}_{k,H}^*$ and an optimal switching sequence $\mathcal{V}_{k,H}^*$. However, the receding horizon approach uses the first element of these sequences only, as described by Eq. (18). According to Eq. (3), when a control update is not received by the actuator node, the actuator keeps applying the last control input.

Remark 2 (Computations)**.** *The online burden in the smart node is limited to fetch data in a lookup table. The size of this table is related to the discretization of the state space used in the offline step. One can adapt the accuracy of the lookup table to the precision needed and the computation resources available online.*

Remark 3 (Explicit MPC)**.** *The value iteration method (which includes an offline step) is different from the so-called explicit MPC schemes [30], [31], which consist in solving a sub-optimal or parametrized problem offline in order to lighten the online burden.*

Remark 4 (Packetized Predictive Control)**.** *Since an optimal control sequence over an horizon H has been computed at the smart node side, one may argue that holding the control input at the actuator side is not the best choice when no update is received and when the time elapsed since the last update was received is less than the horizon length. Alternatively, one may use other elements of the control sequence at the actuator side (as suggested by works such as [32]). With this, the smart node would have to send the whole sequence, which would imply a consequent energy consumption, which is precisely what we want to avoid. On the other hand, applying the other elements of the control sequence may result in better open-loop performance, which may in turn extend the time spent without updating the control sequence.*

The current formulation could be extended to encompass such packetized transmissions *without major difficulties. Note however that the switched system as given in Eq.* (4) *would have to be modified accordingly. In particular, the dimension of the switched system should be augmented by $H-1$ to keep the memory of the H control inputs in the sequence.*

IV. Stability analysis

This section investigates the stability of the closed-loop system designed in Section III-C. Our stability analysis is based on the framework of Input-to-State Stability (ISS), and relies on the works [33], [34]. A general approach to global ISS for discrete-time systems can be found in [33]. The authors in [34] extend the general approach to consider constraints on the state space and the control space, and introduce the notion of Input-to-State practical Stability (ISpS), meaning that the system converges to a bounded invariant set rather than to a point.

ISS is often used to examine the stability of a system despite the presence of disturbances. Here, we use it in a different context, where the difficulty comes from the, at times, open-loop operation when transmissions are interrupted to save energy. We analyze stability of the state x only. Indeed, the $\tilde{u}$ term in the state is a memory of the applied inputs and hence its stability does not need to be assessed directly. It follows from the one of x. The radio mode m, which can only take a finite number of values, may not be converging to a particular mode, but this does not prevent the state x to be bounded. The results given in [33], [34] must be adapted to our setup where we are dealing with stability of part of the state only.

We will need the following notation and definitions:

- A function $\alpha(s) : \mathbb{R}_{\geq 0} \to \mathbb{R}_{\geq 0}$ is a $\mathcal{K}$-function, or of class $\mathcal{K}$, if it is continuous, strictly increasing and $\alpha(0) = 0$. If moreover $\alpha(s) \to \infty$ as $s \to \infty$, then $\alpha(s)$ is a $\mathcal{K}_\infty$-function, or of class $\mathcal{K}_\infty$.
- A function $\gamma(s, k) : \mathbb{R}_{\geq 0} \times \mathbb{Z}_{\geq 0} \to \mathbb{R}_{\geq 0}$ is said to be a $\mathcal{KL}$-function, or of class $\mathcal{KL}$, if for each fixed $k \geq 0$, $\gamma(\cdot\,, k)$ is of class $\mathcal{K}$, and for each fixed $s \geq 0$, $\gamma(s, \cdot\,)$ is decreasing, and $\gamma(s, k) \to 0$ as $k \to \infty$.
- $\alpha^{-1}(s)$ denotes, when it exists, the inverse of a function $\alpha(s)$.
- $\alpha_1 \circ \alpha_2(s) \triangleq \alpha_1(\alpha_2(s))$ denotes the composition of two functions $\alpha_1(s)$ and $\alpha_2(s)$.
- $\mathrm{id}(s)$ is the identity function, *i.e.*, $\mathrm{id}(s) = s,\ \forall s$.

We are interested in the stability of the closed-loop state trajectories of system (1) with the policy (18) and arbitrary

initial conditions $(z_0, m_0) = (x_0, \tilde{u}_0, m_0)$. The system evolves as follows:

$$\begin{cases} z_{k+1} = f_{v_k^*}(z_k(x_0, \tilde{u}_0, m_0), u_k^*) \\ m_{k+1} = v_k^* = \eta^*(z_k, m_k) \\ u_k^* = \mu^*(z_k, m_k). \end{cases} \tag{19}$$

We consider the following notion of Global Input-to-State practical Stability (GISpS).

Definition 1. *The closed-loop system* (19) *is said to be GISpS if there exist a $\mathcal{KL}$-function γ and a (finite) constant $c \geq 0$, such that, for any initial condition $(x_0, \tilde{u}_0, m_0) \in \mathbb{X}$,*

$$\|x_k\| \leq \gamma(\|x_0\|, k) + c, \quad k \in \mathbb{Z}_{\geq 0}. \tag{20}$$

Notice that this definition describes Input-to-State practical stability only for the x term in the state (*i.e.*, amounts to a form of *partial stability*). In particular, if the closed-loop system (19) is GISpS, as stated in Definition 1, then for any $\epsilon > 0$ and for any initial condition, there exists a finite time $\bar{k}$ (depending on the initial condition and on ϵ) such that $\|z_k\| \leq c + \epsilon$ for all $k \geq \bar{k}$; this can be easily inferred from Eq. (20) and the fact that $\gamma(\|z_0\|, k) \to 0$ as $k \to \infty$. As far as the $\tilde{u}$ term is concerned, recall from Eq. (2) that this is a memory of the previously-applied control inputs, which is updated whenever a transmitting decision is taken, and kept constant otherwise. When it is updated, it is a linear function of the x term in the state, so that if we prove that x is bounded, then also $\tilde{u}$ is bounded.[4] The mode m takes values in a finite set, and we are not concerned with its convergence: it might settle to a constant value or keep varying, without preventing convergence of x.

We will prove that the closed-loop system (19) is GISpS. To do so, we will make use of the following notion of Lyapunov-like function.

Definition 2. *$V : \mathbb{X} \to \mathbb{R}_{\geq 0}$ is called a GISpS-Lyapunov function for the system* (19) *if*

1) *there exist a pair of $\mathcal{K}_\infty$-functions α_1, α_2, and a constant $c_1 \geq 0$ such that, for all $((x, \tilde{u}), m) \in \mathbb{X}$:*

$$\alpha_1(\|x\|) \leq V((x, \tilde{u}), m) \leq \alpha_2(\|x\|) + c_1 \tag{21}$$

2) *there exist a suitable $\mathcal{K}_\infty$-function α_3 and a constant $c_2 \geq 0$ such that, for all $((x, \tilde{u}), m) \in \mathbb{X}$:*

$$\begin{aligned} \Delta V((x, \tilde{u}), m) &\triangleq V(f_{v^*}((x, \tilde{u}), u^*), v^*) - V((x, \tilde{u}), m) \\ &\leq -\alpha_3(\|x\|) + c_2. \end{aligned} \tag{22}$$

Our stability result is subject to a condition on the final weighting factor Q_F in Eq. (7), as stated in the following assumption.

Assumption 3. *The weighting factor Q_F in Eq.* (7) *is positive definite, and there exists $\kappa \in \mathbb{R}^{n_u \times (n_x + n_u)}$ such that $\max\{|\operatorname{eigs}(\Phi_{CL} - \Gamma_{CL}\kappa)|\} \leq 1$ and $Q'_F \succeq 0$, where*

$$\begin{aligned} Q'_F \triangleq Q_F - (\Phi_{CL} - \Gamma_{CL}\kappa)^\top Q_F (\Phi_{CL} - \Gamma_{CL}\kappa) - Q_{CL} \\ - \kappa^\top R_{CL} \kappa. \end{aligned} \tag{23}$$

[4]For nonlinear systems this aspect becomes more subtle, see [35].

Assumption 3 is akin to the so-called *terminal cost* inequality that can be found in finite horizon optimization problems, and is discussed for instance in [36]. Note that the existence of the gain κ is only used in the definition of Assumption 3; this gain is not necessarily used afterwards as the closed-loop feedback gain. The following result establishes GISpS of the system of interest.

Theorem 1. *Suppose that Assumption 3 holds. Then the closed-loop* (19) *is GISpS.*

Proof. See the appendix. □

Since the cost function penalizes transmission energy (and thereby does not use closed-loop control when the system state is small), asymptotic stability of the origin cannot be achieved in general. The best one can hope for is stability of a bounded set, as established in Theorem 1. The situation is akin to that encountered in sparse control formulations, such as [37].

V. Simulation studies

We simulate the proposed control and radio-mode switching scheme on a second-order plant. We focus on an unstable plant because energy-efficiency is more critical in the case where the system is not converging naturally. We consider the following system

$$\dot{x}(t) = \begin{bmatrix} 0 & 1 \\ -2 & 3 \end{bmatrix} x(t) + \begin{bmatrix} 0 \\ 1 \end{bmatrix} u(t)$$

discretized with sampling period $T_s = 0.05$s. We consider three radio-modes with the transition costs described in Example 1. In the definition of the cost-to-go (Eq. (5)), we fix $\bar{Q} = 0.1\, I$, $\bar{R} = 0.1$, while we use α as a design parameter, to explore different tradeoffs between control cost and energy. In our optimization, to find the optimal policy, we consider an optimization horizon $H = 10$, and a terminal cost

$$Q_F = \begin{bmatrix} 1.5 & 0 & 0 \\ 0 & 1.5 & 0 \\ 0 & 0 & 0.1 \end{bmatrix}.$$

We want to examine the energy savings obtained by the introduction of the low consuming mode `Idle` (mode 2) in between `Tx` (mode 1) and `Sleep` (mode 3). To this end, we run simulations using three modes, and compare them with simulations with only two modes, *i.e.*, using only `Tx` and `Sleep`. An example of simulation (with $\alpha = 2$) is shown in Figure 3. The system is stabilized in both cases, as shown by the state trajectories in Figure 3(a), with a similar control performance (upper curve in Figure 3(b)). The energy cost used to obtain a similar control performance is lower when using three modes (lower curve in Figure 3(b)), particularly in the second part of the simulation, after the system has reached the invariant set around its equilibrium point. Figure 3(c) illustrates the switching decisions for the radio mode. In the time interval of 20s shown in the figure, the total number of transmissions is the same for both schemes: 53 transmissions and 347 non-transmissions; the `Idle` mode was used 57 times in the 3-modes scheme. Notice that it is quite natural to have a similar number of transmissions, but in general there is no guarantee to have exactly the same number, because the

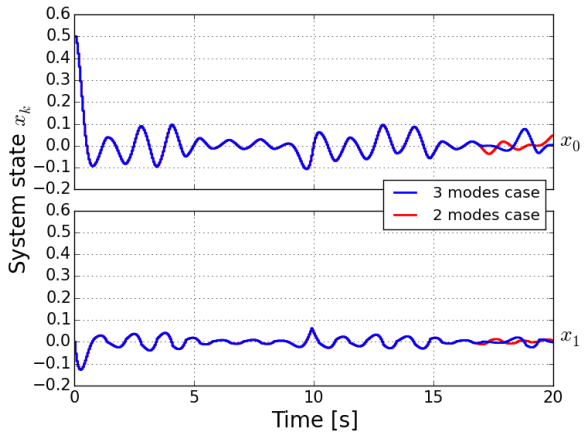

(a) Controlled system state x_k. The first component is plotted above, and the second below.

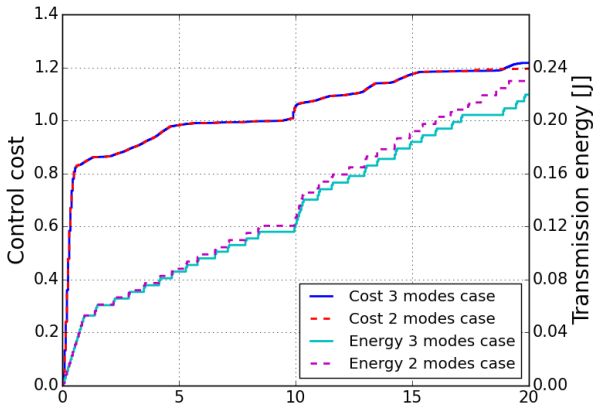

(b) Accumulated control cost $\sum_{i=0}^{k}(x_i^\top \bar{Q} x_i + u_i^\top \bar{R} u_i)$ and energy consumption (in Joules) $E_k = \sum_{i=1}^{k} \theta_{m_{i-1},m_i}$.

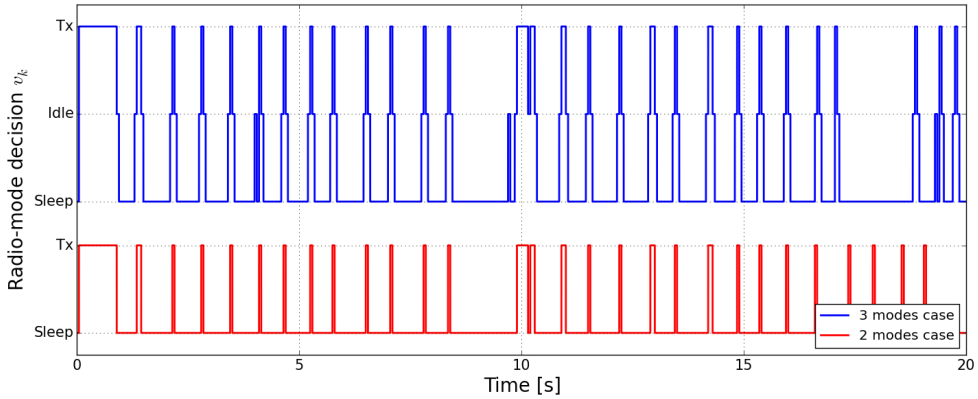

(c) Switching decision v_k.

Fig. 3. Online simulations comparing the cases with two and three radio modes.

joint optimization of control and radio-mode might lead to different transmission decisions in the two cases. The total energy consumption of the radio chip is of 215.62 mJ for the 3-modes scheme, which improves upon the 226.22 mJ of the 2-modes schemes; clearly, transmitting at all times would have required a much higher energy, of 1157.1 mJ.

Figure 4 illustrates different tradeoffs between total control cost $\sum_{i=0}^{k_f}(x_i^\top \bar{Q} x_i + u_i^\top \bar{R} u_i)$ and energy consumption $E_{k_f} = \sum_{i=1}^{k_f} \theta_{m_{i-1},m_i}$, obtained with different values of α in the cost-to-go definition in Eq. (5). Both costs are cumulative over the simulation horizon of 20 s. Points in the plots are obtained averaging over 16 different initial conditions for the state z, and over all initial radio-modes.

In Figure 4(a), we can see that better tradeoffs are obtained by using three modes rather than only two, thus showing the interest of using an additional `Idle` mode.

In Figure 4(b), we compare our technique with a case where two modes (`Tx` and `Sleep`) are used in a periodic manner, namely a control input is transmitted once every p time steps, and the control is held constant until next transmission; we use LQR control for the resulting periodic system. For $p = 1$, this is classic LQR control with transmissions at every time step, so clearly this method obtains the best possible control cost, but at the price of high energy cost for transmissions. Other values of p lead to tradeoffs which are significantly worse than the ones obtained when optimizing the transmission pattern, either with two or with three modes.

We would like to emphasize that, as mentioned in Remark 2, the optimization problem can be run offline, since the problem is time-invariant. Online, the choice of the new radio-mode and of the control gain are functions of the current state only, and can be encoded in look-up tables. To give a pictorial representation of such functions, we consider a 1-dimensional system (1), so that we can use a color-code to represent them. Our example is the system $x_{k+1} = 1.074x_k - 1.4808u_k$, with time step duration $T_s = 0.05$ s, parameters of the cost-to-go $\bar{Q} = 0.01$, $\bar{R} = 0.1$, $\alpha = 1$, and the optimization horizon is $H = 10$; radio-modes are the three ones from Example 1. Figure 5 shows the new radio-mode and the control gain (for the cases when the radio-mode is `Tx`), as a function of current $x, \tilde{u}, m$.

VI. Conclusion

We have presented an energy-efficient joint control law and radio-mode switching policy for a networked control system

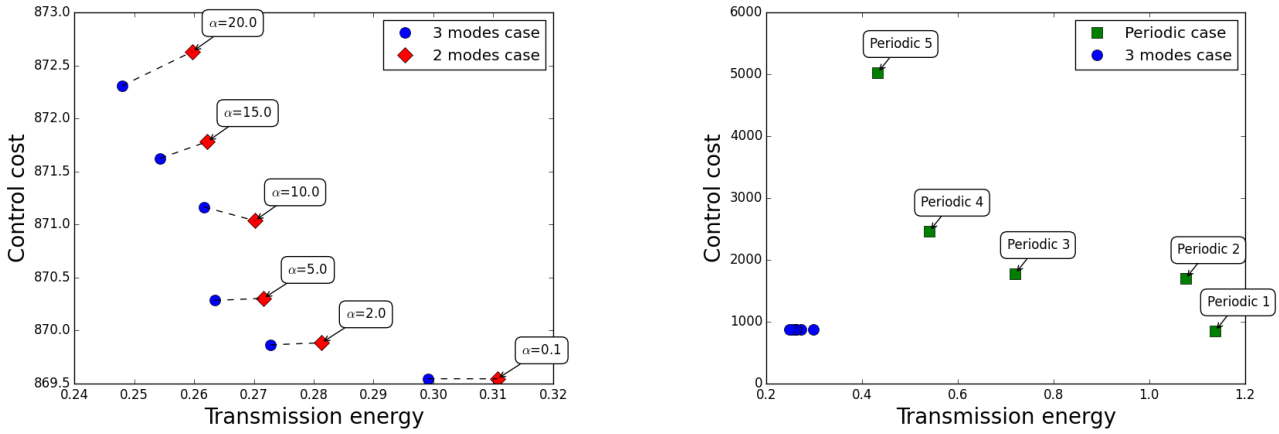

(a) Three modes vs. two modes.

(b) Three modes optimization vs. periodic LQR.

Fig. 4. Different energy/control cost tradeoffs obtained with our method and with periodic transmissions once every p time steps. Accumulated control cost is $\sum_i (x_i^\top \bar{Q} x_i + u_i^\top \bar{R} u_i)$ and total energy consumption (in Joules) is $\sum_i \theta_{m_{i-1},m_i}$.

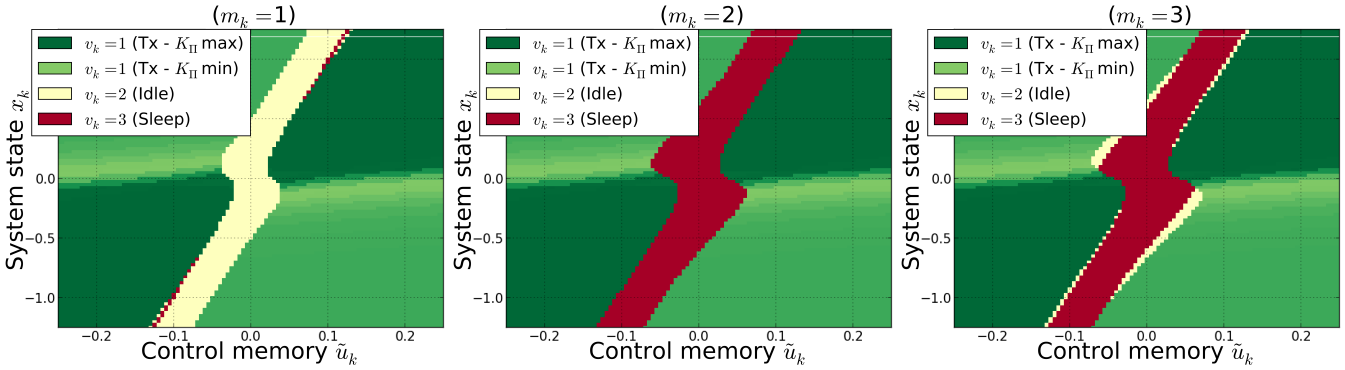

Fig. 5. Color illustration of the optimal control policies, for a scalar system. As a function of current state x (vertical axis), control memory $\tilde{u}$ (horizontal axis) and mode (left, center, or right plot), one obtains the optimal next mode (`Tx` if green, `Idle` if yellow, `Off` if red), and the value of the control gain in case the mode is `Tx` (depicted with intensity of green color).

architecture which comprises a smart sensor node in charge of computing the control updates. In order to save energy at the smart node, at each sampling instant, the smart sensor node decides whether or not to send an optimal control update. When running open loop, the smart node decides among several low-consuming radio-modes depending on the current level of awareness that is needed by the smart node. All these choices are made by evaluating the future impact of current decisions in terms of energy-transition costs and control performance. These decisions involve a trade-off between energy consumption and control performance. The control law and the switching policy are derived jointly in the framework of optimal control and solved using dynamic programming and value iteration methods. The stability of the proposed method has been elucidated in the framework of practical Input-to-State Stability.

Future directions include the extension to a stochastic case where communication failures are taken into account. Here one could study the use of several transmission power levels that can be used to increase the success probability of the transmission, at the price of consuming more energy, cf. [12].

A much more challenging extension would be to take into account a distributed architecture involving several smart nodes. Indeed, within our framework, the derivation of the optimal control law relies on the assumption that the smart node has exact knowledge of not only the state of the system, but also of its evolution regarding its own choice. When considering several sensors, this assumption does not necessarily hold, and new techniques need to be devised.

Another possible extension is to consider a nonlinear system. This is again very challenging, since optimal control of nonlinear systems is very difficult even in the absence of energy issues, while here we are building upon the explicit solution of LQR.

Appendix
Proof of Theorem 1

Our subsequent analysis is inspired by [33], [34]. Authors in [33] consider asymptotic stability to a point, while authors in [34] consider practical stability but they introduce constraints on the state or control spaces that we do not consider. The current setup has the particularity to consider an ISpS-Lyapunov function depending on x, $\tilde{u}$ and m while the practical stability is limited to x.

A. Preliminaries

To prove Theorem 1, we will first introduce the following preliminary technical result:

Lemma 2. *If the system* (19) *admits a GISpS-Lyapunov function, then it is GISpS.*

Proof. This proof is based on the proofs of ISS and ISpS in [33], [34]. We assume that Eqs. (21)-(22) hold, *i.e.*, that the system (19) admits an GISpS-Lyapunov function, denoted $V(z,m)$. Let's prove that the closed-loop system is GISpS in the sense of Definition 1. The proof is divided into three steps: first we prove that the closed-loop system admits an invariant set[5]; then we show that the invariant set is attractive; finally we establish that having an attractive invariant set is equivalent to practical stability.

Step 1: Finding an invariant set $\Omega \subset \mathbb{X}$.

We define $\overline{\alpha}_2(s) \triangleq \alpha_2(s) + s$. Noting that $c_1 \geq 0$, $\|x\| \geq 0$ and α_2 is increasing, Eq. (21) implies

$$V((x,\tilde{u}),m) \leq \alpha_2(\|x\| + c_1) + \|x\| + c_1 = \overline{\alpha}_2(\|x\| + c_1).$$

Hence,

$$\overline{\alpha}_2^{-1}(V((x,\tilde{u}),m)) \leq \|x\| + c_1. \tag{24}$$

Let $\xi(s)$ be a $\mathcal{K}_\infty$-function. If $c_1 \leq \|x\|$, then $\frac{\|x\|+c_1}{2} \leq \|x\|$, which implies

$$\alpha_3\left(\frac{\|x\| + c_1}{2}\right) \leq \alpha_3(\|x\|) \leq \alpha_3(\|x\|) + \xi(c_1).$$

If $c_1 > \|x\|$, similarly we obtain

$$\xi\left(\frac{\|x\| + c_1}{2}\right) \leq \xi(c_1) \leq \alpha_3(\|x\|) + \xi(c_1).$$

Introducing the function

$$\underline{\alpha_3}(s) \triangleq \min\left\{\xi\left(\frac{s}{2}\right), \alpha_3\left(\frac{s}{2}\right)\right\},$$

we have just proved that

$$\underline{\alpha_3}(\|x\| + c_1) \leq \alpha_3(\|x\|) + \xi(c_1), \ \forall x. \tag{25}$$

Notice that $\underline{\alpha_3}$ is a $\mathcal{K}_\infty$-function, and in particular is increasing, so that Eqs. (24) and (25) imply

$$\underline{\alpha_3}\left(\overline{\alpha}_2^{-1}(V((x,\tilde{u}),m))\right) \leq \alpha_3(\|x\|) + \xi(c_1).$$

If we introduce

$$\alpha_4 \triangleq \underline{\alpha_3} \circ \overline{\alpha}_2^{-1},$$

then we have

$$\alpha_4\left(V((x,\tilde{u}),m)\right) \leq \alpha_3(\|x\|) + \xi(c_1).$$

By Eq. (22), this gives

$$\begin{aligned}\Delta V((x,\tilde{u}),m) &\leq -\alpha_3(\|x\|) + c_2 - \xi(c_1) + \xi(c_1) \\ &\leq -\alpha_4\left(V((x,\tilde{u}),m)\right) + c_2 + \xi(c_1). \end{aligned} \tag{26}$$

[5]A set $\Omega \subset \mathbb{X}$ is called an invariant set for system (19) if any $(z,m) \in \Omega$ verifies $\left(f_{\eta^*(z,m)}(z,\mu^*(z,m)),\eta^*(z,m)\right) \in \Omega$.

Let ρ be a $\mathcal{K}_\infty$-function such that $(\mathrm{id} - \rho)$ is also a $\mathcal{K}_\infty$-function; for example, we can consider $\rho(s) = s/2$. We define $\omega \triangleq \alpha_4^{-1} \circ \rho^{-1}$ and $c_3 \triangleq c_2 + \xi(c_1)$, and the set

$$\Omega \triangleq \{(z,m) \in \mathbb{X} : V(z,m) \leq \omega(c_3)\}. \tag{27}$$

We assume that $(\mathrm{id} - \alpha_4)$ is a $\mathcal{K}_\infty$-function. This assumption is not restrictive, since Lemma B.1 in [33] proves that, in case $(\mathrm{id} - \alpha_4)$ is not $\mathcal{K}_\infty$, there exists a $\mathcal{K}_\infty$-function $\hat{\alpha}_4$ such that $\hat{\alpha}_4(s) \leq \alpha_4(s)$ and $(\mathrm{id} - \hat{\alpha}_4)$ is $\mathcal{K}_\infty$, so that $\hat{\alpha}_4$ can be used instead of α_4 in the rest of this proof.

Let's consider $(z,m) \in \Omega$. From Eq.(26) , we get

$$V(f_{v^*}(z,u^*),v^*) - V(z,m) \leq -\alpha_4\left(V(z,m)\right) + c_3,$$

and hence

$$V(f_{v^*}(z,u^*),v^*) \leq (\mathrm{id} - \alpha_4)\left(V(z,m)\right) + c_3.$$

Since $(\mathrm{id} - \alpha_4)$ is increasing and $(z,m) \in \Omega$, this implies

$$\begin{aligned} V(f_{v^*}(z,u^*),v^*) &\leq (\mathrm{id} - \alpha_4)\left(\omega(c_3)\right) + c_3 \\ &= \omega(c_3) - \rho^{-1}(c_3) + c_3 = \omega(c_3) - (\mathrm{id} - \rho)(\rho^{-1}(c_3)). \end{aligned}$$

Since $(\mathrm{id} - \rho)$ is a $\mathcal{K}_\infty$-function, $(\mathrm{id} - \rho)(\rho^{-1}(c_3)) \geq 0$, thus showing that

$$V(f_{v^*}(z,u^*),v^*) \leq \omega(c_3),$$

which establishes that Ω is an invariant set for the closed-loop system (19).

Step 2: Proving that the invariant set Ω is attractive.

We want to prove that, for any $(z_k,m_k) \notin \Omega$, there exists a finite $\bar{k} \geq k$ such that $(z_{\bar{k}},m_{\bar{k}}) \in \Omega$. Consider the trajectory which at time k is in (z_k,m_k), and let $\bar{k} \geq k$ be the first time where this trajectory enters Ω. Having already proved that Ω is an invariant set, clearly $\bar{k} > k$, $(z_h,m_h) \notin \Omega$ for all $h < \bar{k}$ and $(z_h,m_h) \in \Omega$ for all $h \geq \bar{k}$. Notice that $\bar{k}$ is possibly infinite (in case the trajectory never enters Ω) and our goal is indeed to prove that $\bar{k}$ is finite.

For all $h < \bar{k}$, $(z_h,m_h) \notin \Omega$ means that

$$V(z_h,m_h) > \omega(c_3) = \alpha_4^{-1} \circ \rho^{-1}(c_3),$$

thereby,

$$\rho \circ \alpha_4(V(z_h,m_h)) > c_3. \tag{28}$$

Moreover, by Eq. (26),

$$\Delta V(z_h,m_h) \leq -\alpha_4\left(V(z_h,m_h)\right) + c_3,$$

which can be re-written as follows:

$$-(\mathrm{id} - \rho) \circ \alpha_4\left(V(z,m)\right) - \rho \circ \alpha_4\left(V(z,m)\right) + c_3,$$

so that, by Eq. (28),

$$\Delta V(z,m) \leq -(id - \rho) \circ \alpha_4\left(V(z,m)\right). \tag{29}$$

Eq. (29) holds for all z_h, m_h with $0 \leq h < \bar{k}$; notice that $(id - \rho) \circ \alpha_4$ is a $\mathcal{K}_\infty$-function. According to [38, Lemma 4.3], this implies that there exists a $\mathcal{KL}$-function $\hat{\gamma}(s,h)$ such that

$$V(z_h,m_h) \leq \hat{\gamma}(V(z_0,m_0),h), \ \forall h < \bar{k}. \tag{30}$$

Now, when considering fixed z_0, m_0 (as we are looking at one trajectory), $\gamma(V(z_0,m_0),h)$ is a decreasing function of h, which tends to 0 for $h \to \infty$. Without loss of generality,[6] let

[6]Since $\omega(c_3) = \alpha_4^{-1} \circ \rho^{-1}(\xi(c_1) + c_2)$, $\omega(c_3) \geq 0$. If $\omega(c_3) = 0$, then $c_1 = c_2 = 0$. We can instead consider $\tilde{c}_1, \tilde{c}_2 > 0$.

us assume that $\omega(c_3) > 0$. Hence, there exists a finite time $\bar{k}$ such that, for all $h \geq \bar{t}$, $\gamma(V(z_0, m_0), h) \leq \omega(c_3)$ and hence also $V(z_h, m_h) \leq \omega(c_3)$, *i.e.*, $(z_h, m_h) \in \Omega$, thus completing the proof that Ω is an attractive set.

Step 3: Proving that Eq. (20) holds.

Eq. (21) implies that $\|x_k\| \leq \alpha_1^{-1}(V((x_k, \tilde{u}_k), m_k))$. Since α_1^{-1} is increasing, we shall use bounds on $V((x_k, \tilde{u}_k), m_k)$.

If $((x_k, \tilde{u}_k), m_k) \in \Omega$, by definition of Ω, it holds that $V((x_k, \tilde{u}_k), m_k) \leq \omega(c_3)$, and hence $\|x_k\| \leq \alpha_1^{-1}(\omega(c_3))$.

If $((x_k, \tilde{u}_k), m_k) \notin \Omega$, then we have proved that $V((x_k, \tilde{u}_k), m_k) \leq \hat{\gamma}\left(V((x_0, \tilde{u}_0), m_0), k)\right)$ for a suitable $\mathcal{KL}$-function $\hat{\gamma}$ (see Eq. (30)), so that

$$\|x_k\| \leq \alpha_1^{-1}(\gamma\left(V((x_0, \tilde{u}_0), m_0), k)\right)).$$

From this, we will look for a looser but more useful bound. Eq. (21) implies that $V((x_0, \tilde{u}_0), m_0) \leq \alpha_2(\|x_0\|) + c_1$, which gives

$$\|x_k\| \leq \alpha_1^{-1}\left(\hat{\gamma}\left(\alpha_2(\|x_0\|) + c_1, k\right)\right). \tag{31}$$

Notice that, for fixed k, $\alpha^{-1}\left(\hat{\gamma}\left(s, k\right)\right)$ is a $\mathcal{K}_\infty$-function in the variable s. For any function $\sigma(s)$ of class $\mathcal{K}_\infty$, if $s_1 \geq s_2$, then $\alpha(s_1 + s_2) \leq \alpha(2s_1)$, while if $s_1 \leq s_2$, then $\alpha(s_1 + s_2) \leq \alpha(2s_2)$, and hence, in both cases,

$$\alpha(s_1 + s_2) \leq \alpha(2s_1) + \alpha(2s_2).$$

Applying this bound to the function $\alpha^{-1}\left(\hat{\gamma}\left(s, k\right)\right)$ in Eq. (31), we obtain

$$\|x_k\| \leq \alpha_1^{-1}\left(\hat{\gamma}\left(2\alpha_2(\|x_0\|), k\right)\right) + \alpha_1^{-1}\left(\hat{\gamma}\left(2c_1, k\right)\right).$$

The function $\alpha_1^{-1}\left(\hat{\gamma}\left(2c_1, k\right)\right)$ is of class $\mathcal{K}_\infty$; in particular, being decreasing, it attains its maximum for $k = 0$, which gives

$$\|x_k\| \leq \alpha_1^{-1}\left(\hat{\gamma}\left(2\alpha_2(\|x_0\|), k\right)\right) + \alpha_1^{-1}\left(\hat{\gamma}\left(2c_1, 0\right)\right). \tag{32}$$

Recalling that we have obtained Eq. (32) for all $((x_k, \tilde{u}_k), m_k) \notin \Omega$, while the cost $V((x_k, \tilde{u}_k), m_k) \leq \omega(c_3)$ for all $((x_k, \tilde{u}_k), m_k) \in \Omega$, we can conclude that for all $((x_k, \tilde{u}_k), m_k)$ we can bound $\|x_k\|$ by the sum of these two bounds. This shows that

$$\|x_k\| \leq \gamma(\|x_0\|, k) + c,$$

with $\gamma(s, k) = \alpha_1^{-1}\left(\hat{\gamma}\left(2\alpha_2(s), k\right)\right)$ and

$$c = \alpha_1^{-1}\left(\hat{\gamma}\left(2c_1, 0\right)\right) + \alpha_1^{-1}\left(\omega(c_3)\right).$$

This proves Lemma 2. □

Having established that if the system admits a GISpS-Lyapunov function, then it is stable in the sense of Definition 1, we will next prove Theorem 1, by showing that a GISpS-Lyapunov function exists for our closed-loop system.

B. Proof of Theorem 1

Now we want to prove that the system (19) is GISpS. We will first show that, under the stated conditions, the system (19) admits a GISpS-Lyapunov function; by Lemma 2, this implies that it is GISpS. Our proof is in three steps, one for each of the inequalities in Definition 2. As a candidate Lyapunov function, we take the value function $V_H(z, m) = J_H^*(z, m)$, whose characterization is in Lemma 1. Before starting the proof, it is convenient to make the following observation about matrices Π involved in this characterization: Looking at the definition of $\mathcal{P}_i$, we can notice that if $(\Pi, \boldsymbol{\pi}) \in \mathcal{P}_{H-i}^{(2)}$ (equivalently, if $v_{k+i}^* \neq 1$), then Π is positive definite, while if $(\Pi, \boldsymbol{\pi}) \in \mathcal{P}_{H-i}^{(1)}$ (*i.e.*, $v_{k+i}^* = 1$), then Π is positive semi-definite, and more precisely

$$\Pi = \begin{bmatrix} \Pi_x & 0 \\ 0 & 0 \end{bmatrix},$$

where Π_x is of size $n_x \times n_x$ and positive definite.

Step 1: Proving that there exists α_1 of class $\mathcal{K}_\infty$ such that $\alpha_1(\|x\|) \geq V_H(z, m)$, where $z = (x, \tilde{u})$.

We consider the expression for V_H given in Lemma 1, and in particular Eq. (17). We note that $\theta_{ij} \geq 0,\ \forall (i, j) \in \mathbb{M}^2$ implies that $\pi_v \geq 0,\ \forall v \in \mathbb{M},\ \forall (\Pi, \boldsymbol{\pi}) \in \mathcal{P}_H$. Hence,

$$\begin{aligned} V_H(z, m) &\geq \min_{(\Pi, \boldsymbol{\pi}) \in \mathcal{P}_H} \left\{ z^\top \Pi z \right\} \\ &= \min \left\{ \min_{(\Pi, \boldsymbol{\pi}) \in \mathcal{P}_H^{(1)}} z^\top \Pi z, \min_{(\Pi, \boldsymbol{\pi}) \in \mathcal{P}_H^{(2)}} z^\top \Pi z \right\}. \end{aligned}$$

Let's consider the two minima separately: For all Π in the first minimization we have $\Pi = \left[\begin{smallmatrix} \Pi_x & 0 \\ 0 & 0 \end{smallmatrix}\right]$ with positive definite Π_x. Then,

$$\min_{(\Pi, \boldsymbol{\pi}) \in \mathcal{P}_H^{(1)}} z^\top \Pi z \geq \lambda_1 \|x\|^2,$$

where $\lambda_1 > 0$ is the minimum of the eigenvalues of all the blocks Π_x for matrices appearing in $\mathcal{P}_H^{(1)}$. All Π in the second minimization are positive definite; letting $\lambda_2 > 0$ be the minimum of their eigenvalues, we have

$$\min_{(\Pi, \boldsymbol{\pi}) \in \mathcal{P}_H^{(2)}} z^\top \Pi z \geq \lambda_2 \|z\|^2 \geq \lambda_2 \|x\|^2,$$

which leads to the bound:

$$V_H(z, m) \geq \min\{\lambda_1, \lambda_2\} \|x\|^2 \triangleq \alpha_1(\|x\|),$$

as desired.

Step 2: Proving that there exists α_2 of class $\mathcal{K}_\infty$ and a constant c_1 such that $V_H(z, m) \leq \alpha_2(\|x\|) + c_1$, where $z = (x, \tilde{u})$.

We look again at Lemma 1, Eq. (17). Clearly, for any fixed $(\Pi, \pi) \in \mathcal{P}_H$,

$$V_H(z, m) \leq z^\top \Pi z + \pi_m.$$

Then, notice that $\pi_m \leq H \alpha \theta_{\max}$, where

$$\theta_{\max} \triangleq \max_{i, j \in \mathbb{M}} \{\theta_{i,j}\}.$$

Hence,

$$V_H(z, m) \leq z^\top \Pi z + H \alpha \theta_{\max}.$$

Now notice that $\mathcal{P}_H = \mathcal{P}_H^{(1)} \cup \mathcal{P}_H^{(2)}$ and that $\mathcal{P}_H^{(1)}$ is non-empty. Thus, we can choose Π being in $\mathcal{P}_H^{(1)}$ and thereby having the structure $\Pi = \left[\begin{smallmatrix} \Pi_x & 0 \\ 0 & 0 \end{smallmatrix}\right]$. This gives

$$z^\top \Pi z \leq \lambda_{\max} \|x\|^2,$$

where $\lambda_{\max}$ is the largest eigenvalue of Π. Consequently, we have

$$V_H(z, m) \leq \alpha_2(\|x\|) + c_1,$$

with $\alpha_2(\|x\|) \triangleq \lambda_{\max}\|x\|^2$ and $c \triangleq H\alpha\theta_{\max}$.

Step 3: Proving that there exists α_3 of class $\mathcal{K}_\infty$ and a constant c_2 such that $\Delta V_H(z,m) \leq -\alpha_3(\|x\|) + c_2$.

We need to find an upper bound to

$$\Delta V_H(z_k, m_k) = V_H(z_{k+1}, m_{k+1}) - V_H(z_k, m_k),$$

where $(z_{k+1}, m_{k+1}) = \big(f_{v_k^*}(z_k, u_k^*), v_k^*\big)$.

Notice that

$$\begin{aligned} V_H(z_{k+1}, m_{k+1}) &= J_H^*(z_{k+1}, m_{k+1}) \\ &= \min_{\mathcal{U}_{k+1,H}, \mathcal{V}_{k+1,H}} J_H(z_{k+1}, m_{k+1}, \mathcal{U}_{k+1,H}, \mathcal{V}_{k+1,H}). \end{aligned}$$

Hence, if we take a particular policy

$$(\mathcal{U}_{k+1,H}, \mathcal{V}_{k+1,H}) = (\bar{\mathcal{U}}_{k+1,H}, \bar{\mathcal{V}}_{k+1,H}),$$

which might not be the optimal one, then it holds that

$$V_H(z_{k+1}, m_{k+1}) \leq J_H(z_{k+1}, m_{k+1}, \bar{\mathcal{U}}_{k+1,H}, \bar{\mathcal{V}}_{k+1,H}). \quad (33)$$

We consider the following policy:

$$\begin{aligned} \bar{\mathcal{U}}_{k+1,H} &\triangleq (u_{k+1}^*, u_{k+2}^*, \dots, u_{k+H-1}^*, \bar{u}_{k+H}) \\ \bar{\mathcal{V}}_{k+1,H} &\triangleq (v_{k+1}^*, v_{k+2}^*, \dots, v_{k+H-1}^*, \bar{v}_{k+H}), \end{aligned} \quad (34)$$

where $\bar{v}_{k+H} = 1$ and $\bar{u}_{k+H} = -\bar{\kappa} z_{k+H}$ with $\bar{\kappa}$ chosen such that Assumption 3 is satisfied. In Eq. (34), the terms u_i^* and v_i^* are taken from the optimal policy from time k over an horizon H, *i.e.*, $\mathcal{U}_{k,H}^* = (u_k^*, u_{k+1}^*, \dots, u_{k+H-1}^*)$ and $\mathcal{V}_{k,H}^* = (v_k^*, v_{k+1}^*, \dots, v_{k+H-1}^*)$. With this choice, it is easy to see that

$$\begin{aligned} &J_H(z_{k+1}, m_{k+1}, \bar{\mathcal{U}}_{k+1,H}, \bar{\mathcal{V}}_{k+1,H}) \\ &\quad = V_H(z_k, m_k) - \ell_{v_k^*}(z_k, m_k, u_k^*) - z_{k+H}^\top Q_F z_{k+H} \\ &\qquad + \ell_1(z_{k+H}, m_{k+H}, \bar{u}_{k+H}) + z_{k+H+1}^\top Q_F z_{k+H+1}. \end{aligned}$$

This, together with Eq. (33), gives

$$\begin{aligned} \Delta V_H(z_k, m_k) &\leq -\ell_{v_k^*}(z_k, m_k, u_k^*) - z_{k+H}^\top Q_F z_{k+H} \\ &\quad + \ell_1(z_{k+H}, m_{k+H}, \bar{u}_{k+H}) + z_{k+H+1}^\top Q_F z_{k+H+1}. \end{aligned} \quad (35)$$

We recall that $\bar{v}_{k+H} = 1$ and $\bar{u}_{k+H} = -\bar{\kappa} z_{k+H}$, so that $z_{k+H+1} = (\Phi_{CL} - \Gamma_{CL}\bar{K}) z_{k+H}$. Considering the latter and the definition of the cost-to-go ℓ_1 (see Eq. (5)), we obtain

$$\begin{aligned} \ell_1(z_{k+H}, m_{k+H}, \bar{u}_{k+H}) &= z_{k+H}^\top Q_{CL} z_{k+H} \\ &\quad + z_{k+H}^\top \bar{\kappa}^\top R_{CL} \bar{\kappa} z_{k+H} + \alpha\theta_{m_{k+H},1} \end{aligned}$$

and

$$\begin{aligned} &z_{k+H+1}^\top Q_F z_{k+H+1} \\ &\quad = z_{k+H}^\top \left(\Phi_{CL} - \Gamma_{CL}\bar{\kappa}\right)^\top Q_F (\Phi_{CL} - \Gamma_{CL}\bar{\kappa}) \, z_{k+H}, \end{aligned}$$

so that Eq. (35) can be re-written as follows:

$$\begin{aligned} \Delta V_H(z_k, m_k) &\leq -\ell_{v_k^*}(z_k, m_k, u_k^*) - z_{k+H}^\top Q'_F z_{k+H} \\ &\quad + \alpha\theta_{m_{k+H},1}, \end{aligned}$$

where we have used the definition of Q'_F, see Eq. (23). By Assumption 3, $Q'_F \succeq 0$, and trivially

$$\theta_{m_{k+H},1} \leq \theta_{\max} \triangleq \max_{i,j \in \mathbb{M}} \{\theta_{i,j}\}.$$

Hence,

$$\Delta V_H(z_k, m_k) \leq -\ell_{v_k^*}(z_k, m_k, u_k^*) + \alpha\theta_{\max}.$$

Recalling the definition of the stage cost in (6), and noting that $R_{v_k^*} \succeq 0$, we have

$$\Delta V_H(z_k, m_k) \leq -z_k^\top Q_{v_k^*} z_k - \alpha\theta_{\min} + \alpha\theta_{\max},$$

where

$$\theta_{\min} \triangleq \min_{i,j \in \mathbb{M}} \{\theta_{i,j}\}.$$

Now notice that $z_k^\top Q_{v_k^*} z_k$ is equal to $x_k^\top \bar{Q} x_k$ when $v_k^* = 1$, and equal to $x_k^\top \bar{Q} x_k + \tilde{u}_k^\top \bar{R} \tilde{u}_k \geq x_k^\top \bar{Q} x_k$ when $v_k^* = 1$. Finally, letting $\lambda > 0$ be the smallest eigenvalue of $\bar{Q}$, we obtain

$$\Delta V_H(z_k, m_k) \leq -\lambda\|x\|^2 + \alpha(\theta_{\max} - \theta_{\min}),$$

from where the result follows.

REFERENCES

[1] J. Hespanha, P. Naghshtabrizi, and Y. Xu, "A survey of recent results in networked control systems," *Proceedings of the IEEE*, vol. 95, no. 1, pp. 138–162, Jan. 2007.

[2] L. H. Correia, D. F. Macedo, A. L. dos Santos, A. A. Loureiro, and J. M. S. Nogueira, "Transmission power control techniques for wireless sensor networks," *Computer Networks*, vol. 51, no. 17, pp. 4765–4779, 2007.

[3] R. Jurdak, A. Ruzzelli, and G. O'Hare, "Adaptive radio modes in sensor networks: How deep to sleep?" in *5th IEEE Communications Society Conference on Sensor, Mesh and Ad Hoc Communications and Networks, SECON'08*, June 2008, pp. 386–394.

[4] M. I. Brownfield, T. Nelson, S. Midkiff, and N. J. Davis, "Wireless sensor network radio power management and simulation models," *The Open Electrical & Electronic Engineering Journal*, vol. 4, pp. 21–31, 2010.

[5] G. Nair, F. Fagnani, S. Zampieri, and R. Evans, "Feedback control under data rate constraints: An overview," *Proceedings of the IEEE*, vol. 95, no. 1, pp. 108–137, Jan. 2007.

[6] W. Heemels, K. Johansson, and P. Tabuada, "An introduction to event-triggered and self-triggered control," in *IEEE Conference on Decision and Control (CDC) 2012, Hawaii, USA*, December 2012, pp. 3270–3285.

[7] M. Miskowicz, Ed., *Event-Based Control and Signal Processing*. CRC Press, 2015.

[8] X. Liu and A. Goldsmith, "Wireless network design for distributed control," in *43rd IEEE Conference on Decision and Control*, vol. 3, Dec. 2004, pp. 2823–2829.

[9] N. Cardoso de Castro, C. Canudas de Wit, and K. H. Johansson, "On energy-aware communication and control co-design in wireless networked control systems," in *2nd IFAC Workshop on Estimation and Control of Networked Systems, NecSys'10*, 2010.

[10] P. Park, C. Fischione, A. Bonivento, K. Johansson, and A. Sangiovanni-Vincentelli, "Breath: A self-adapting protocol for wireless sensor networks in control and automation," in *5th Annual IEEE Communications Society Conference on Sensor, Mesh and Ad Hoc Communications and Networks*, June 2008, pp. 323–331.

[11] P. D. Marco, P. Park, C. Fischione, and K. H. Johansson, "Trend: a timely, reliable, energy-efficient dynamic wsn protocol for control application." in *IEEE International Conference on Communications*, 2010.

[12] D. E. Quevedo, J. Østergaard, and A. Ahlén, "Power control and coding formulation for state estimation with wireless sensors," *IEEE Trans. Contr. Syst. Technol.*, vol. 22, no. 2, pp. 413–427, Mar. 2014.

[13] N. Cardoso de Castro, C. Canudas de Wit, and F. Garin, "Energy-aware wireless networked control using radio-mode management," in *American Control Conference ACC'12, Montréal, Canada*, 2012.

[14] N. Cardoso de Castro, F. Garin, and C. Canudas de Wit, *Information and Control in Networks*. Springer, 2014, ch. Optimal Radio-Mode Switching for Wireless Networked Control, pp. 87–119.

[15] P. Park, J. Araujo, and K. Johansson, "Wireless networked control system co-design," in *2011 IEEE International Conference on Networking, Sensing and Control (ICNSC)*, April 2011, pp. 486–491.

[16] J. Araujo, M. Mazo, A. Anta, P. Tabuada, and K. Johansson, "System architectures, protocols and algorithms for aperiodic wireless control systems," *IEEE Transactions on Industrial Informatics*, vol. 10, no. 1, pp. 175–184, 2014.

[17] A. Anta and P. Tabuada, "To sample or not to sample: Self-triggered control for nonlinear systems," *IEEE Trans. Automatic Control*, vol. 55, no. 9, pp. 2030–2042, 2010.

[18] B. Demirel, Z. Zou, P. Soldati, and M. Johansson, "Modular design of jointly optimal controllers and forwarding policies for wireless control," *IEEE Trans. Automatic Control*, vol. 59, no. 12, pp. 3252–3265, 2014.

[19] N. Cardoso de Castro, D. E. Quevedo, F. Garin, and C. Canudas de Wit, "Smart energy-aware sensors for event-based control," in *51st IEEE Conference on Decision and Control CDC'12,*, Dec. 2012, pp. 7224–7229.

[20] D. E. Quevedo, V. Gupta, W. Ma, and S. Yüksel, "Stochastic stability of event-triggered anytime control," *IEEE Trans. Automat. Contr.*, vol. 59, no. 12, pp. 3373–3379, Dec. 2014.

[21] W. Heemels, M. Donkers, and A. Teel, "Periodic event-triggered control for linear systems," *IEEE Transactions on Automatic Control*, vol. 58, pp. 847–861, April 2013.

[22] Chipcon Products, *CC1100 Low-Power Sub- 1 GHz RF Transceiver*, Texas Instruments.

[23] J. Rawlings and D. Mayne, *Model Predictive Control Theory and Design*. Nob Hill Pub., 2009.

[24] L. Grüne and J. Pannek, *Nonlinear Model Predictive Control: Theory and Algorithms*. Springer, 2011.

[25] R. E. Bellman, *Dynamic Programming*. Princeton University Press, 1957.

[26] D. P. Bertsekas, *Dynamic Programming and Optimal Control*, M. A. S. Belmont, Ed., 2005, vol. 1.

[27] D. Görges, M. Izak, and S. Liu, "Optimal control and scheduling of switched systems," *IEEE Transactions on Automatic Control*, vol. 56, no. 1, pp. 135–140, Jan. 2011.

[28] A. Eqtami, D. Dimarogonas, and K. Kyriakopoulos, "Event-triggered control for discrete-time systems," in *American Control Conference (ACC), 2010*, 2010, pp. 4719–4724.

[29] D. Lehmann, E. Henriksson, and K. Johansson, "Event-triggered model predictive control of discrete-time linear systems subject to disturbances," in *Control Conference (ECC), 2013 European*, 2013, pp. 1156–1161.

[30] A. Bemporad, M. Morari, V. Dua, and E. N. Pistikopoulos, "The explicit linear quadratic regulator for constrained systems," *Automatica*, vol. 38, no. 1, pp. 3 – 20, 2002.

[31] A. Alessio and A. Bemporad, "A survey on explicit model predictive control," in *Nonlinear Model Predictive Control*, 2009, vol. 384, pp. 345–369.

[32] D. E. Quevedo and D. Nešić, "Robust stability of packetized predictive control of nonlinear systems with disturbances and Markovian packet losses," *Automatica*, vol. 48, no. 8, pp. 1803–1811, Aug. 2012.

[33] Z.-P. Jiang and Y. Wang, "Input-to-state stability for discrete-time nonlinear systems," *Automatica*, vol. 37, no. 6, pp. 857 – 869, 2001.

[34] D. M. Raimondo, D. Limón, M. Lazar, L. Magni, and E. Camacho, "Min-max Model Predictive Control of Nonlinear Systems: A Unifying Overview on Stability," *European Journal of Control*, vol. 15, no. 1, pp. 5–21, Jan. 2009.

[35] M. Lješnjanin, D. E. Quevedo, and D. Nešić, "Packetized MPC with dynamic scheduling constraints and bounded packet dropouts," *Automatica*, vol. 50, no. 3, pp. 784—797, Mar. 2014.

[36] J. W. Lee, "Exponential stability of constrained receding horizon control with terminal ellipsoid constraints," *IEEE Trans. Automat. Contr.*, vol. 45, no. 1, pp. 83–88, 2000.

[37] M. Nagahara, D. E. Quevedo, and J. Østergaard, "Sparse packetized predictive control for networked control over erasure channels," *IEEE Trans. Automat. Contr.*, vol. 59, no. 7, pp. 1899–1905, 2014.

[38] Z.-P. Jiang and Y. Wang, "A converse Lyapunov theorem for discrete-time systems with disturbances," *Systems & Control Letters*, vol. 45, no. 1, pp. 49–58, Jan. 2002.